Appl. Phys. B 85, 55–58 (2006)
DOI: 10.1007/s00340-006-2337-4

Applied Physics B
Lasers and Optics

W. LIU✉
F. THÉBERGE
J.-F. DAIGLE
P.T. SIMARD
S.M. SARIFI
Y. KAMALI
H.L. XU
S.L. CHIN

An efficient control of ultrashort laser filament location in air for the purpose of remote sensing

Centre d'Optique, Photonique et Laser (COPL), and Département de Physique, de Génie Physique et d'Optique, Université Laval, Québec, Québec G1K 7P4, Canada

Received: 10 March 2006/Revised version: 1 May 2006
Published online: 1 July 2006 •

ABSTRACT The unavoidable hot spots in a practical terawatt level laser pulse will self-focus in air at a short distance. The short distance cannot be changed significantly by only controlling the chirp or divergence. We overcome such early self-focusing by using a telescope, which enlarges the diameter of the beam, thus that of the hot spots. The telescope's effective focal length is much shorter than the self-focusing distance of both the enlarged beam and the hot spots. Then, the resulting filaments merge into the geometrical focus whose position is controllable by the telescope. This technique also minimizes the generation of white light.

PACS 52.38.Hb; 42.65.Jx; 52.35.Mw

1 Introduction

It has been foreseen that pollutant detection in the atmosphere will be one of the most promising applications of the filamentation phenomenon [1, 2]. It is due to the fact that after the filamentation process, an intense ultrashort laser pulse self-transforms into a new light source with stunning characteristics, such as ultrabroad spectrum bandwidth (white light laser [3], from 230 nm to 4 μm [4, 5]) and fairly high intensity (intensity clamping [6, 7], in air, it is $\sim 5 \times 10^{13}$ W/cm^2). Accompanying the occurrence of the filamentation, a plasma channel, which is normally referred to as 'filament' [8], is left behind by the laser pulse. Therefore, with a light detection and ranging (Lidar) technique, the pollutants in the atmosphere can be identified through recording their fingerprint fluorescence spectra emitted following the plasma recombination process [2]. This proposal has been successfully confirmed by using ethanol vapour as a tentative contaminants [9].

Another recent work [10] has demonstrated that the maximum contrast between the fluorescence signal and backscattered white light background [11] can be found at the beginning of the filament. Thus, to ensure the sensitivity of remote pollutant detection, it is necessary to control the filaments and have the filamentation occurring at a desired distance as far as kilometers in the atmosphere. This knowledge will be helpful for the remote laser-induced breakdown spectroscopy using filamentation [12, 13] and the generation of the third harmonic light at a remote distance too [14, 15]. However, though experimental observation of filaments at 2 km distance in the atmosphere has been reported [16], the ability to consistently control the filament location over long distances and to distinguish the plasma fluorescence from the white light background are still an experimental challenges. For example, we found in our previous experiments that despite the effort of changing the initial chirp and divergence of the beam, there were difficulties in moving the filaments more than 50 m away from the output of our laser system [10]. A similar result has been reported in [17], where the filament could be moved away to a maximum distance of 250 m by chirping the pulse to 6 ps. But more lengthening of the pulse would not help to move further the filaments. We suspect that this phenomenon is due to the effect of the commonly existed small hot spots in a terawatt (TW) level laser beam profile. Because the hot spots may contain powers exceeding the critical power for self-focusing (a few gigawatts (GW) in air) and their sizes are considerably small, they can easily lead to the filament formation at a short distance. The distance is normally much shorter than the one predicted according to the whole beam diameter.

In this letter we discuss an inexpensive and efficient way to solve this problem. Essentially, we let our laser beam pass through a telescope. This telescope serves two purposes. First, it is convenient to achieve a variable effective focal length by changing the distance between the divergent and convergent optical components. The other, and more important, is to enlarge the laser beam diameter, hence that of the hot spots. It will be shown that by this technique, the impact of the hot spots on the filament formation is minimized. It gives rise to a better control of the filament location over a long distance.

2 Experiment and results

The experimental setup is shown in Fig. 1. Our telescope consists of a 5 cm diameter convex mirror, whose focal length is −50 cm, and a focusing lens with focal length of 100 cm (diameter of 8 cm). The focusing lens was installed on a computer controlled motorized stage, allowing us to change the effective focal length of the telescope. For convenience, an effective focal length D will be cited in the fol-

✉ Fax: (418)6562623, E-mail: Weiwei.liu.1@ulaval.ca

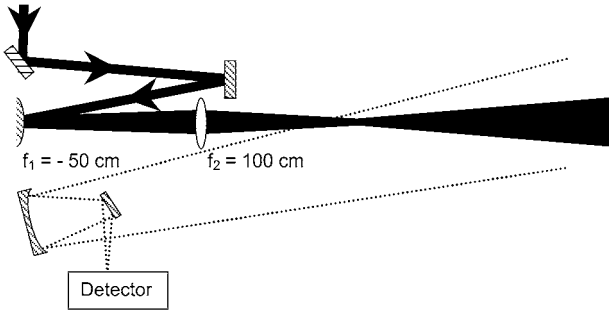

FIGURE 1 Experimental setup

lowing discussions to denote the distance between the convex mirror and the geometrical focus of the telescope. Its value can be easily calculated according to the displacement between the convex mirror and the focusing lens.

After the telescope, the laser beam diameter was increased from 1.2 cm at full width at half maximum (FWHM) to about 2.5 cm (FWHM). The laser spectrum was centered at 800 nm. The pulse energy was fixed at 40 mJ/pulse and the duration was negatively chirped to 2 ps. The laser pulse was sent through a 100 m long corridor [10]. Since its peak power (20 GW) was significantly higher than the critical power of self-focusing ($\sim$ 5 GW [18]), filamentation occurred inside the corridor. Then, the backscattered light was collected by a typical Lidar setup [10] and sent to a photomultiplier tube (PMT). A 0° dielectric mirror (made of fused silica) with high reflectivity at 800 nm and an interference filter centered at 337 nm, which corresponds to the strongest line of the nitrogen fluorescence [19], were placed in front of the PMT in order to isolate the fluorescence signal from the other radiations. The PMT signal was monitored on an oscilloscope. The recorded fluorescence signal indicated the location of the filament [10].

A few examples of the waveforms are exhibited in Fig. 2 for different values of D. These waveforms were averaged over 10 shots. The horizontal coordinate has been calibrated to be the propagation distance inside the corridor. The origin is the position of the convex mirror. Figure 2 follows closely the result discussed in [10] where it was shown that the fluorescence signal is strongly localized in space. It also clearly demonstrates that the position of the signal, i.e., filament, can be continuously moved with respect to the change of the effective focal length from $D = 6.4$ m in Fig. 2a to $D = 91.7$ m in Fig. 2e. Note that the displacement of the fluorescence signal illustrated in Fig. 2c–e has overcome the barrier of 50 m encountered in our previous experiments with smaller beam sizes [10]. In fact, we found that in this work the moving distance of the filament was only limited by the total length of the corridor.

We, furthermore, plot the peak positions of the signal measured in our experiment versus the distance D in Fig. 3 (open triangles). For the sake of helping the observation, we have also drawn in Fig. 3 a solid line, whose slope is equal to 1 and implies the exact coincidence of the signal peaks with the geometrical foci. It can be seen that the experimental measurement nicely follows the solid line. Only a small deviation could be noticed at the long distance ($D > 70$ m). The slight discrepancy is associated with the self-focusing and could be

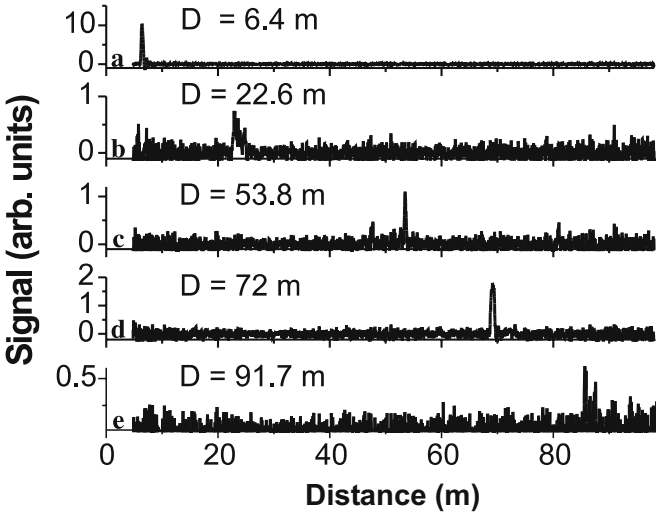

FIGURE 2 Lidar collected 337 nm signals as function of the distance inside the corridor for different sending telescope configurations. D indicates the distance between the convex mirror ($f = -50$ cm) and the calculated geometrical focus position

seen later (1). Figure 3 reveals that the filament location is mainly governed by the geometrical focus. At the same time, the inset of Fig. 3 shows how the signal peak value evolves when the filament is moved to different distances. The signal has been corrected by the geometrical factors of our Lidar system, including the overlap function and distance dependence [10]. The curve in the insert panel in Fig. 3 initially undergoes a steep decrease up to 30 m and shows almost invariable signal after 30 m. We note that there is a modulation of the result in the range from 60 m to 80 m. It could be explained by the presence of a strong ventilation exit near that region [20]. The tendency sketched in the inset of Fig. 3 is in good agreement with a recent work [21], which concludes that the plasma density inside the filament will decrease significantly with the increase of the external focal length. But if the

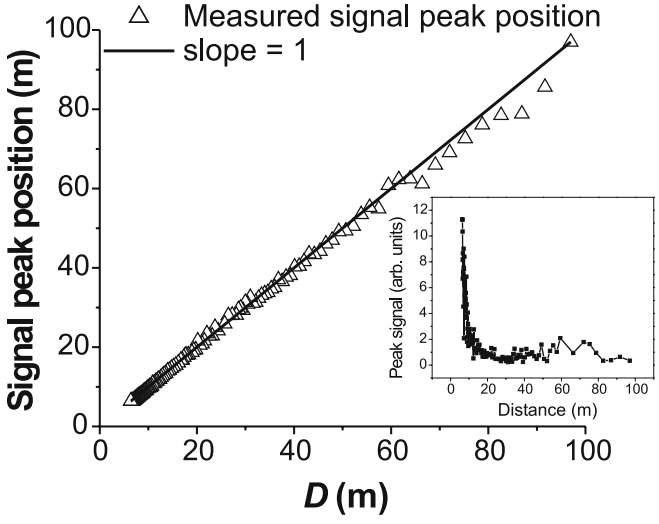

FIGURE 3 Comparison between the measured fluorescence peak position (*open triangles*) and the calculated geometrical focus (*solid line*). *Inset*: The signal peak value changes with respect to variable effective focal length of the telescope

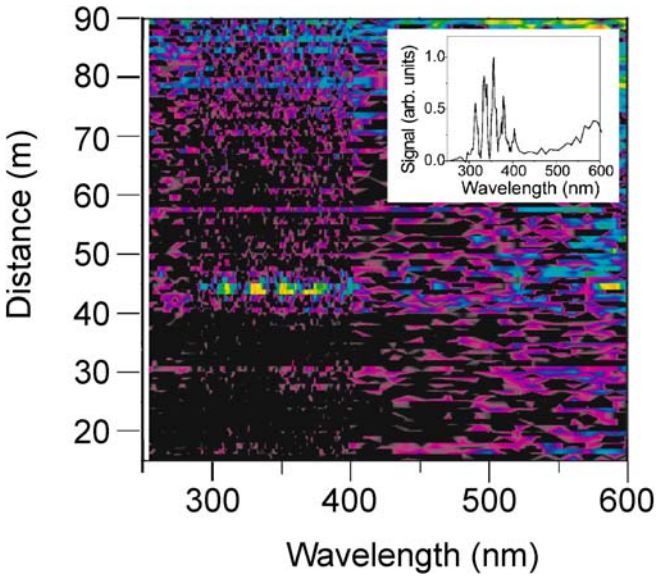

FIGURE 4 2-dimension spectrum recorded by Lidar when $D = 45$ m. The *inset* highlights the spectrum at 45 m

external focal length is long enough, the plasma density will be independent to the focal length, so does the fluorescence signal [21].

Evidently, the insert panel in Fig. 3 is opposite to the linear optics principle, according to which the focus intensity is inversely proportional to the square of the focal length. For instance, if only geometrical focusing played the role in our experiments, to produce the similar laser peak intensity as the one during the filamentation process ($\sim 5 \times 10^{13}$ W/cm^2), would require a laser energy of 18 J/pulse when $D = 100$ m. Apparently, this result given by the plain geometrical simplification is far away from the reality. This argument firmly confirms it is indeed the self-focusing that gives rise to high laser intensity and induce fluorescence signal.

In the experiment, we also coupled the Lidar collected backscattered light into a spectrometer (Acton, SpecPro-500i) and used the PMT as its detector to investigate the spectral distribution as function of the propagation distance [10]. The studied wavelength covered from 250 nm to 600 nm. The obtained two-dimensional (2D) spectrum has been calibrated by the Lidar geometrical factors as well as the spectral response of the PMT and spectrometer. The result is depicted in Fig. 4 for $D = 45$ m. Unlike the previous spectrum in [10], very little white light contamination is observed in Fig. 4. This feature is outlined by an inset which shows the acquired spectrum at 45 m. Compared with the spectrum reported in [10], the white light signal level has been reduced by orders of magnitude.

3 Discussion

It is well known that in the presence of the external focusing, the self-focusing distance z_f', which is also the starting point of the filament, is determined by [22]:

$$z_f' = \frac{z_f f}{z_f + f}\,, \tag{1}$$

in which f denotes the focal length of the lens and z_f stands for the self-focusing distance for a parallel Gaussian beam given by [23]:

$$z_f = \frac{0.367ka^2}{\left\{\left[(P/P_{cr})^{1/2} - 0.852\right]^2 - 0.0219\right\}^{1/2}}\,, \tag{2}$$

where ka^2 represents the diffraction length of the beam, while P corresponds to the laser peak power and P_{cr} is the critical power for self-focusing. Immediately, we see from (1) that if $z_f \gg f$, then $z_f' \approx f$. Due to the fact that z_f is proportional to the square of the beam radius, increasing the size of the beam is a more efficient way to fulfill $z_f \gg f$ than only reducing the peak power. Related to the current work, a parallel Gaussian beam with diameter of 2.5 cm (FWHM) and 20 GW peak power would self-focus at a distance of about 570 m. On the other hand, we have known from [8] that when the diameter of the same laser beam was squeezed to 6.2 mm (FWHM), the collimated pulse self-focused at 17 m due to the effect of hot spots. This distance can be considered as the effective self-focusing distance of the hot spots. With this as a reference, we can estimate that in the case of 2.5 cm diameter beam, z_f for hot spots would be more than 260 m according to (2). So when D was smaller than 100 m, the condition $z_f \gg f$ was satisfied for both the total beam and hot spots. Hence, we were able to move the filament to any distance inside our 100 m long corridor.

Comparing the current case to propagating a chirped parallel beam [24] or diverging beam with only large diameter [25], the advantage of focusing the laser pulse after enlarging its diameter is significant. In [24, 25], the appearance of intense hot spots across the laser beam profile was used to indicate the formation of the filaments. These hot spots are widely spaced. Our group has recently pointed out that multiple filaments produced by widely spaced hot spot in a larger diameter beam can be weak and unstable. It results in randomly fluctuating fluorescence signal [26]. From the point of view of remotely sensing pollutants in air using the fluorescence technique, this situation needs to be avoided. On the other hand, a smaller diameter beam will most likely lead to strong and consistent fluorescence emission [27] (but the position of the filament cannot be controlled easily because the hot spots tend to self-focus quickly as mentioned above). This phenomenon has been elucidated by the scenario of multiple filaments competition [26]. Since in our experimental scheme the filamentation starts near the geometrical focus and the beam size is small at this position, the competition of multiple filaments will happen in a constructive way [26]. As a result, consistent and strong fluorescence signal shall be guaranteed. This is what we observed in Fig. 2.

It is also easy to notice that a short filament will be expected when the condition of $z_f' \approx f$ is established since the filament length ($L_{filament}$) could be approximated by $L_{filament} \approx f - z_f'$. In the present work, the overall lengths of the filaments are less then 1.5 m even near the end of the corridor. It is much shorter than other reported total length of the filaments in the atmosphere (at least tens meters) [28–30]. Moreover, the self-steepening effect would be considerably reduced in the sense that we used a not-so-short pulse. Taking into account both factors, spectral broadening would be much less pronounced. It leads to the suppressed white light

contamination as shown in Fig. 4. For the first time according to our knowledge, we have reported a white light contamination free backscattered nitrogen fluorescence spectrum in the course of filamentation in an open air environment.

Up to now, we have proved that by a simple telescope technique, we have reached the goal of controlling the filament location over a long distance in air. Based on the intrinsic linear optics concept of (1) we expect that this technique is also applicable to kilometer range. For example, to scale our measurements to 1 km away, using (2) we basically need to expand the laser beam diameter to 8.5 cm (FWHM). That dimension is still reasonable and affordable in practice.

4 Conclusion

In conclusion, we have obtained an effective and reliable method to master the filament location in air. The technique uses a telescope to enlarge the laser beam's diameter in such a way that a parallel beam with the same diameter, as well as those hot spots within the beam, should self-focus at a much longer distance than the effective focal length of the telescope. Under this condition, the resulting filament merges into the geometrical focus, which is adjustable by varying the relative distance between the divergent and convergent optical components. By this scheme, the white light generation is also considerably reduced. The main advantage of the technique also relies on its scalability to kilometer range.

ACKNOWLEDGEMENTS This work was partially supported by NSERC, DRDC-Valcartier, Canada Research Chairs, CIPI, CFI, Femtotech and FQRNT. We appreciate very much the technical assistance of Mr. Mario Martin.

REFERENCES

1 J. Kasparian, M. Rodriguez, G. Méjean, J. Yu, E. Salmon, H. Wille, R. Bourayou, S. Frey, Y.-B. André, A. Mysyrowicz, R. Sauerbrey, J.P. Wolf, L. Wöste, Science **301**, 61 (2003)
2 J.-F. Gravel, Q. Luo, D. Boudreau, X.P. Tang, S.L. Chin, Anal. Chem. **76**, 4799 (2004)
3 S.L. Chin, A. Brodeur, S. Petit, O.G. Kosareva, V.P. Kandidov, J. Nonlinear Opt. Phys. Mater. **8**, 121 (1999)
4 F. Théberge, W. Liu, Q. Luo, S.L. Chin, Appl. Phys. B **80**, 221 (2005)
5 J. Kasparian, R. Sauerbrey, D. Mondelain, S. Niedermeier, J. Yu, J.P. Wolf, Y.-B. Andre, M. Franco, B. Prade, S. Tzortzakis, A. Mysyrowicz, M. Rodriguez, H. Wille, L. Wöste, Opt. Lett. **25**, 1397 (2000)
6 J. Kasparian, R. Sauerbrey, S.L. Chin, Appl. Phys. B **71**, 877 (2000)
7 A. Becker, N. Aközbek, K. Vijayalakshmi, E. Oral, C.M. Bowden, S.L. Chin, Appl. Phys. B **73**, 287 (2001)
8 S.L. Chin, S.A. Hosseini, W. Liu, Q. Luo, F. Théberge, N. Aközbek, A. Becker, V.P. Kandidov, O.G. Kosareva, H. Schroeder, Can. J. Phys. **83**, 863 (2005)
9 Q. Luo, H.L. Xu, S.A. Hosseini, J.-F. Daigle, F. Théberge, M. Sharifi, S.L. Chin, Appl. Phys. B **82**, 105 (2005)
10 F. Théberge, W. Liu, S.A. Hosseini, Q. Luo, S.M. Sharifi, S.L. Chin, Appl. Phys. B **81**, 131 (2005)
11 J. Yu, D. Mondelain, G. Ange, R. Volk, S. Niedermeier, J.P. Wolf, J. Kasparian, R. Sauerbrey, Opt. Lett. **26**, 533 (2001)
12 A. Ting, I. Alexeev, D. Gordon, E. Briscoe, J. Peñano, R. Hubbard, P. Sprangle, G. Rubel, Appl. Opt. **44**, 5315 (2005)
13 K. Stelmaszczyk, P. Rohwetter, G. Méjean, J. Yu, E. Salmon, J. Kasparian, R. Ackermann, J.P. Wolf, L. Wöste, Appl. Phys. Lett. **85**, 3799 (2004)
14 N. Aközbek, A. Iwasaki, A. Becker, M. Scalora, S.L. Chin, C.M. Bowden, Phys. Rev. Lett. **89**, 143 901 (2002)
15 F. Théberge, Q. Luo, W. Liu, S.A. Hosseini, M. Sharifi, S.L. Chin, Appl. Phys. Lett. **87**, 081 108 (2005)
16 M. Rodriguez, R. Bourayou, G. Méjean, J. Kasparian, J. Yu, E. Salmon, A. Scholz, B. Stecklum, J. Eislöffel, U. Laux, A.P. Hatzes, R. Sauerbrey, L. Wöste, J.P. Wolf, Phys. Rev. E **69**, 036 607 (2004)
17 G. Méchain, C. D'Amico, Y.-B. André, S. Tzortzakis, M. Franco, B. Prade, A. Mysyrowicz, A. Couairon, E. Salmon, R. Sauerbrey, Opt. Commun. **247**, 171 (2005)
18 W. Liu, S.L. Chin, Opt. Express **13**, 5750 (2005)
19 A. Talebpour, M. Abdel-Fattah, S.L. Chin, Opt. Commun. **183**, 479 (2000)
20 Q. Luo, J. Yu, S.A. Hosseini, W. Liu, B. Ferland, G. Roy, S.L. Chin, Appl. Opt. **44**, 391 (2005)
21 F. Théberge, W. Liu, P.T. Simard, A. Becker, S.L. Chin, Phys. Rev. E (2006), unpublished
22 V.I. Talanov, JETP **11**, 199 (1970)
23 J.H. Marburger, Prog. Quantum Electron. **4**, 35 (1975)
24 H. Wille, M. Rodriguez, J. Kasparian, D. Mondelain, J. Yu, A. Mysyrowicz, R. Sauerbrey, J.P. Wolf, L. Wöste, Eur. Phys. J. Appl. Phys. **20**, 183 (2002)
25 Z. Jin, J. Zhang, M.H. Xu, X. Lu, Y.T. Li, Z.H. Wang, Z.Y. Wei, X.H. Yuan, W. Yu, Opt. Express **13**, 10 424 (2005)
26 S.A. Hosseini, Q. Luo, B. Ferland, W. Liu, S.L. Chin, O.G. Kosareva, N.A. Panov, N. Aközbek, V.P. Kandidov, Phys. Rev. A **70**, 033 802 (2004)
27 Q. Luo, S.A. Hosseini, W. Liu, J.-F. Gravel, O.G. Kosareva, N.A. Panov, N. Aközbek, V.P. Kandidov, G. Roy, S.L. Chin, Appl. Phys. B **80**, 35 (2005)
28 A. Braun, G. Korn, X. Liu, D. Du, J. Squier, G. Mourou, Opt. Lett. **20**, 73 (1995)
29 E.T.J. Nibbering, P.F. Curley, G. Grillon, B.S. Prade, M.A. Franco, F. Salin, A. Mysyrowicz, Opt. Lett. **21**, 62 (1996)
30 A. Brodeur, C.Y. Chien, F.A. Ilkov, S.L. Chin, O.G. Kosareva, V.P. Kandidov, Opt. Lett. **22**, 304 (1997)